

J Mot Biot. Author manuscript; available in Pivic 2014 June 24

Published in final edited form as:

J Mol Biol. 2011 October 28; 413(3): 699–711. doi:10.1016/j.jmb.2011.08.049.

Crystal structure of cardiac troponin C regulatory domain in complex with cadmium and deoxycholic acid reveals novel conformation

Alison Yueh Li^{#1,3}, Jaeyong Lee^{#1}, Dominika Borek², Zbyszek Otwinowski², Glen F. Tibbits^{3,4,1}, and Mark Paetzel^{*,1,3}

¹Department of Molecular Biology and Biochemistry, Simon Fraser University, South Science Building, 8888 University Drive, Burnaby, British Columbia, Canada, V5A 1S6

²Department of Biochemistry, University of Texas Southwestern Medical Center at Dallas, 5323 Harry Hines Boulevard, Dallas, TX 75390, USA

- ³ Department of Biomedical Physiology and Kinesiology, Molecular Cardiac Physiology Group, Simon Fraser University, 8888 University Drive, Burnaby, British Columbia, Canada, V5A 1S6
- ⁴ Cardiovascular Sciences, Child and Family Research Institute, 950 West 28th Ave, Vancouver, BC, Canada V5Z 4H4

Summary

The amino-terminal regulatory domain of cardiac troponin C (cNTnC) plays an important role as the calcium sensor for the troponin complex. Calcium binding to cNTnC results in conformational changes that trigger a cascade of events that leads to cardiac muscle contraction. Cardiac NTnC consists of two EF-hand calcium binding motifs, one of which is dysfunctional in binding calcium. Nevertheless, the defunct EF-hand still maintains a role in cNTnC function. For its structural analysis by X-ray crystallography, human cNTnC with wild-type primary sequence was crystallized in a novel crystallization condition. The crystal structure was solved from single wavelength anomalous dispersion method and refined to 2.2 Å resolution. The structure displays several novel features. Firstly, both EF-hand motifs coordinate cadmium ions derived from the crystallization milieu. Secondly, the ion coordination in the defunct EF-hand motif accompanies unusual changes in the protein conformation. Thirdly, deoxycholic acid, also derived from the crystallization milieu, is bound in the central hydrophobic cavity. This is reminiscent of the interactions observed for cardiac calcium sensitizer drugs that bind to the same core region and maintain the 'open' conformational state of calcium bound cNTnC. The cadmium ion coordination

Publisher's Disclaimer: This is a PDF file of an unedited manuscript that has been accepted for publication. As a service to our customers we are providing this early version of the manuscript. The manuscript will undergo copyediting, typesetting, and review of the resulting proof before it is published in its final citable form. Please note that during the production process errors may be discovered which could affect the content, and all legal disclaimers that apply to the journal pertain.

Accession numbers: Coordinates and structure factors have been deposited in the Protein Data Bank with accession number: 3RV5.

[#] These authors contributed equally to this work.

^{© 2011} Elsevier Ltd. All rights reserved.

^{*}Address correspondence to: Dr. Mark Paetzel, Simon Fraser University, Department of Molecular Biology and Biochemistry, South Science Building, 8888 University Drive, Burnaby, British Columbia, Canada V5A 1S6, Tel.: 778-782-4230, Fax.: 778-782-5583, mpaetzel@sfu.ca.

in the defunct EF-hand indicates that this vestigial calcium binding site retains the structural and functional elements that allow it to coordinate a cadmium ion. However, it is a result of, or concomitant with, large and unusual structural changes in cNTnC.

Keywords

Troponin C; EF-hand; cadmium ion coordination; deoxycholic acid; radiation damage

Introduction

Troponin C (TnC) is a regulatory Ca²⁺ binding subunit in the troponin complex that mediates muscle contraction. The troponin complex, which consists of TnC, TnI, and TnT subunits, is located periodically on the thin filaments composed of tropomyosin and actin monomers¹. During muscle contraction, Ca²⁺ binding to the N-terminal domain of TnC (NTnC) initiates a conformational change that exposes its central hydrophobic cavity. A change in the binding interactions by the inhibitory subunit TnI, from the actin monomers to the TnC hydrophobic core, triggers an overall conformational change within the troponin complex. The final outcome is the cross-bridge cycle that results in muscle contraction². NTnC therefore plays the crucial role of a cytosolic Ca²⁺ sensor in skeletal and cardiac muscle function.

NTnC consists of two EF-hand motifs (denoted 1 and 2), which are commonly present in Ca^{2+} binding proteins (Figure 1A). The classical EF-hand motif consists of two alphahelices oriented approximately perpendicularly to one another and linked by a loop that is normally 12 residues $long^3$. The residues at loop positions 1, 3, 5, 7 and 12 are normally involved in the ion coordination⁴ (Figure 1). Canonically, a Ca^{2+} ion is coordinated by seven oxygen atoms in pentagonal bipyramidal geometry. The five equatorial plane ligands from single carbonyl groups at Y, Z, -Y and a bidentate ligand from a glutamate side chain carboxylate at the -Z positions are complemented by two single axial ligands at the X and -X positions.

Two muscle-specific TnC proteins are expressed in vertebrate muscles. Skeletal TnC (sTnC) in fast skeletal muscle and cardiac TnC (cTnC) in cardiac and slow skeletal muscle differ mostly in the primary sequence and Ca^{2+} binding property of the EF 1 ion binding loop of NTnC (Figure 1B). In mammalian cNTnC, the loop sequence deviates from the canonical sequence by insertion of Val28 resulting in the extension of the loop to 13 residues and substitutions of the two normally chelating aspartate residues by the non-polar Leu29 and Ala31 residues $^{5-}$. This results in loss of Ca^{2+} binding function by the loop. The functional EF 2 with canonical loop sequence and a relatively low Ca^{2+} binding affinity ($\sim 10^{5}$ M $^{-1}$) $^{8-}$ is then proposed to act alone as the cytosolic Ca^{2+} sensor for the cardiac troponin complex $^{6-}$.

Nevertheless, NMR studies indicate that there is a structural and dynamic coupling between the two EF-hands that may play a functional role $\frac{9}{2}$. Other evidence also suggests EF 1 has a role in the function of cNTnC. For example, ectothermic species of vertebrates adapted to colder climates have a significantly different sequence in the N-terminal portion of the EF 1 loop (Figure 1B). In trout, the substituted residues Ile28, Gln29, and Asp30 appear to be

responsible for increasing Ca^{2+} affinity that enables trout cardiac function at significantly lower temperatures $\underline{^{10}}$. Interestingly, these substitutions are not observed in certain semitropical ectotherms (e.g. *Anolis carolinensis* or green anole – accession number GI 327265790) which thrive at 25-30°C and exhibit complete identity with human cTnC over the first 60 amino acids. Clearly these substitutions are related to functionality at a given temperature as was postulated. Intriguingly, one of the characteristic substitutions found in the trout and other teleosts (L29Q) is also observed as a mutation in a patient diagnosed with an inherited cardiac muscle disorder known as familial hypertrophic cardiomyopathy (FHC) $\underline{^{12}}$.

Derived from ongoing structural studies, twelve cNTnC structures solved by nuclear magnetic resonance (NMR) spectroscopy and five by X-ray crystallography are currently available in the Protein Data Bank (PDB) (Supplementary table 1). Most of these structures represent cNTnC domain (residues 1-89) in a Ca²⁺-saturated form with Ca²⁺ coordination shown only by EF 2, while no ion coordination is observed in the dysfunctional binding site of EF 1. However, all crystal structures of cNTnC are that of a mutant version with two substitution mutations (C35S and C84S) introduced to prevent the inter- and intra-molecular disulfide bond formation 13. Although the mutant cTnC was shown to have the same functional properties as the wild type *in vitro*, Cys35 is a part of the EF 1 loop and highly conserved phylogenetically in cNTnC (Figure 1B) 11.

To address the lack of crystallographically determined structures of wild-type cNTnC domain, we have over-expressed, purified, and successfully crystallized the human cNTnC domain with the wild-type primary sequence. This was achieved in a novel crystallization condition that contained cadmium sulphate and deoxycholic acid. The crystal structure was then solved from single wavelength anomalous dispersion (SAD) methods and refined to 2.2 Å resolution. Surprisingly, the structure reveals cNTnC in a highly unique conformation, which permits both EF-hand motifs to coordinate cadmium (Cd²⁺) ions in a canonical bipyramidal pentagonal geometry. This unique conformation is also stabilized in part by deoxycholic acid (DXC) bound to the central hydrophobic core cavity. Analysis of the novel ion coordination state by EF 1 demonstrates that the vestigial loop retains structural and functional elements that enable cadmium ion binding. These elements are reminiscent of the versatile non-canonical EF-hand motifs, however, this coordination is achieved as a result of or concomitant with large and unusual structural changes in cNTnC.

Results and Discussion

Structure solution – dealing with radiation damage and pseudosymmetry

The novel crystals of human cNTnC (residues 1-89) with wild-type primary sequence diffracted to 2.2 Å resolution. However, finding a structure solution via anomalous diffraction techniques or molecular replacement methods presented serious challenges due to the presence of translational pseudosymmetry and the heavy dose of X-ray radiation absorbed in the crystal during data collection. The physical deterioration of the crystal during the exposure to the X-ray beam causes not only a gradual decay of diffraction intensities and structure factor amplitudes, but also structural rearrangements in crystal lattice, hindering the phasing procedures and subsequent refinements. The presence of 50

mM Cd²⁺ in the crystallization solution contributed to an increased X-ray absorption without improving the scattering power of the crystal, resulting in an increased rate of radiation damage and additional diffused background. Moreover, the presence of ordered cadmium ions increased the number of heavy atom sites that needed to be identified by direct methods. The number of selenomethionine (Se-Met) and cadmium positions was relatively high, due to the presence of four molecules in the asymmetric unit (ASU). Without pseudotranslational symmetry, these problems could still be solved without much trouble. However, the crystallographic direct methods in their design assume random positions of heavy atoms and are severely handicapped by the presence of pseudotranslational symmetry, which generates a highly non-random pattern of inter-atom distances. The combination of radiation-induced changes, high number of heavy atom scatterers to be found, and translational pseudosymmetry (native Patterson peak height 47.8 % of origin at 0.5, 0.5, 0.5) resulted in a borderline solvable phasing problem. The Se-Met crystal structure was solved by the SAD method from a dataset collected at the selenium peak wavelength (Se-Met Data 1). The structure was then refined to 2.2 Å resolution with the second anomalous dataset that did not initially yield a SAD solution (Se-Met Data 2). Merging statistics for Se-Met dataset 1 used for experimental phasing and Se-Met dataset 2 dataset used for final refinement are shown in Table 1.

The protein crystal has unit cell dimensions of $51.9 \ \text{Å} \times 81.9 \ \text{Å} \times 100.5 \ \text{Å}$ and belongs to the orthorhombic spacegroup $P2_12_12$. The ASU contains four protein chains with 53.5% solvent content and has a Matthews coefficient of $2.7 \ \text{Å}^3 \ \text{Da}^{-1}$. The four chains are denoted as chain A (Asp3-Met85), chain B (Tyr5-Val82), chain C (Asp3-Met85), and chain D (Tyr5-Val82). Missing residues at the N- and C-termini could not be modeled due to a lack of clear electron density. Chains A and B form a dimer with a two-fold non-crystallographic symmetry and are related to another dimer consisting of chains C and D by a translation with a (0.5, 0.5, 0.5) vector exhibiting a translational pseudosymmetry. A total of twenty one cadmium ions, three calcium ions and five deoxycholic acid molecules were modeled with the protein chains. The final refined structure has a R_{factor} of 22.5 % and a R_{free} of 28.1 %. The average B-factor of the structure is $41.3 \ \text{Å}^2$ (Table 1).

An unusual cNTnC conformation stabilized by cadmium binding

The overall conformation of cNTnC revealed in the crystal structure is a pair of EF-hand motifs connected by a linker sequence (Figure 2A). The first EF-hand motif (EF 1), which follows a short α -helix N (residues 4-10), consists of α -helix A (residues 14-31), the ion binding loop 1, and α -helix B (residues 38-47). The second EF-hand motif (EF 2) consists of α -helix C (residues 54-64), the ion binding loop 2, and α -helix D (residues 74-84). The two EF-hand motifs are connected by a linker that spans residues 48-53. All four protein chains in the ASU have similar conformations. The backbone superimposition of the four chains results in a root-mean-square deviation (r.m.s.d) of 0.73 Å. The major discrepancies between the chains occur at the terminal helices and the linker region that connects helix B and helix C.

In comparison to a previously solved crystal structure of human cNTnC in a Ca^{2+} -saturated form (PDB: 1WRK), the structure presented here adopts a very different conformation with

dramatic changes at helix A (Figure 2B and C). Similar changes are also observed in comparison with various NMR structures (Supplementary Figure 1). Firstly, the residues Val28 - Ala31, normally part of a disordered and dysfunctional loop, adopt an α -helical conformation resulting in an extension of helix A at its C-terminal end (Figure 2D). Secondly, unlike the classical EF-hand motif in which the two helices are oriented perpendicularly, helix A is oriented antiparallel to helix B (Figure 2C). This conformation is stabilized in part by van der Waals interactions between the helices. This also obliterates the 2-fold rotational symmetry between the pair of EF-hand motifs which is a common feature in NTnC structures. Finally, loop 1 in EF 1 previously considered to be dysfunctional is coordinating a Cd²⁺ ion.

The electron densities that clearly indicated metal ions being coordinated by both EF 1 and EF 2 were fitted with Cd^{2+} for the following reasons. First, cadmium ions were identified on the anomalous difference map. There were three potential anomalous scatterers in the crystal: selenium from Se-Met, calcium from protein purification solution, and cadmium from crystallization conditions. Se-Met positions were clearly defined by Se-Met residues. There were 21 other peaks outside of the anomalous peaks describing Se-Met positions. At the data collection wavelength, the cadmium anomalous signal is 3.4 times larger than the signal arising from calcium. The observed signal was thus only consistent with cadmium, as it was too strong to originate from calcium ions. Second, a Cd^{2+} ion has an ionic radius of 0.97 Å, which is very close to that of Ca^{2+} (0.99 Å) and can be coordinated by TnC without causing much perturbation to its overall conformation. Third, in the binding loop of EF 1, one of the coordinating ligand is sulphur from Cys35 and other examples of Cd^{2+} coordination frequently involve cysteine residue 21. Finally the refinement statistics agree with the Cd^{2+} ions present at these sites (Table 1).

 Cd^{2+} ions are also found outside the ion binding loops. An extra Cd^{2+} ion is present in close proximity of every Cd^{2+} -coordinating loop with residues from the loop contributing to its interaction. Cd^{2+} ions are also found between protein chain interfaces and they contribute to the inter chain crystal packing contacts. For example, one Cd^{2+} is coordinated by both Cys35 of Chain A and the carboxylate side chains of Glu15 and Glu19 from its symmetry related counterpart, and another Cd^{2+} is coordinated by Glu32 of chain B and Glu15 of chain C. A total of twenty one Cd^{2+} ions are found at the binding loops and the protein chain interfaces. Their complex coordination networks stabilize the unusual conformation of cNTnC and maintain the critical protein contacts within the protein crystal.

Cadmium coordination by EF 1 and EF 2

All four cNTnC protein chains in the ASU coordinate a Cd^{2+} ion in the binding loop of EF 1. In three chains (Chains A, B, and D), Cd^{2+} coordination adopts canonical seven-ligand pentagonal bipyramidal geometry (Figure 3A). The remaining chain C coordinates Cd^{2+} in six-ligand octahedral geometry for reasons discussed below. Only four residues, Gly30, Asp33, Cys35, and Glu40 supply the coordinating ligands. The five equatorial plane ligands are Asp33 $O^{\delta 1}$ (Y) and $O^{\delta 2}$ (Z), Cys35 O (-Y), and Glu40 $O^{\epsilon 1}$ and $O^{\epsilon 2}$ (-Z). These are complemented by two axial ligands, Gly30 O (X) and Cys35 S (-X) (Table 2).

The Cd^{2+} coordination state at the ion binding loop of EF 2 is identical in all four cNTnC molecules of the ASU. It adopts the canonical seven-ligand pentagonal bipyramidal coordination with ligands from five conserved residues: Asp65 (X), Asp67 (Y), Ser69 (Z), Thr71 (-Y), and Glu76 (-Z) and one water molecule (-X) (Figure 3B). The coordinating ligands are listed in Table 2. The ligands and backbone conformation of the loop is virtually identical to the Ca^{2+} coordination by EF 2 in other cTnC structures. The backbone of the coordinating loop region (Asp65-Glu76) aligns with a root-mean-square deviation (r.m.s.d) of 0.4 Å with $1J1E^{2-}_{-2}$ 0.3 Å with $1WRK^{2-}_{-3}$. The similarity of calcium and cadmium coordination has previously been corroborated by other calcium binding proteins such as calbindin D9k that displays comparable coordination of Cd^{2+} in solution to that of Ca^{2+} $\frac{24}{-}$.

Comparison of the loop sequences (Figure 3C) shows that the absence of two chelating glutamate residues in the N-terminal part of loop 1 does not permit ion coordination by the same canonical conformation as in loop 2. Instead, loop 1 has compensated for the difference by adopting a novel backbone fold and coordination characteristics to fulfil the canonical geometry.

The first novel characteristic is that the carboxylate group of Asp33 is in a planar orientation to the equatorial plane of Cd^{2+} and ligand interactions. Canonically an aspartate residue in the equivalent position contributes only one oxygen atom from its carboxylate group and occupies a single Z position. However, in the structure presented here, the Asp33 bidentate ligand occupies both Y and Z coordination positions in chains A, B and D. In chain C, Asp33 does not occupy both positions and because of this, the Cd^{2+} coordination fails to adopt the canonical geometry. We are not aware of any other examples of one aspartate residue providing bidentate ligands for both Y and Z positions.

A second unique characteristic is the ion coordination shown by Cys35. Normally, the equivalent residue supplies the backbone carbonyl atom for only the –Y ligand position. In the structure presented here, as well as the backbone carbonyl, the sulphur side chain atom of Cys35 is involved in ion coordination at –X ligand position, which is normally occupied by a water molecule. We could not find another example of an EF-hand motif that utilizes cysteine as one of the coordinating ligands. The extra coordination may be due to the nature of the bound ion. Chemically Cd²⁺ is a soft metal ion and would preferentially coordinate soft atoms such as sulphur²⁵. However, Ca²⁺, which is a hard metal ion would not normally prefer sulphur as a ligand.

The final and the most striking characteristic is the coordination by the Gly30 carbonyl oxygen in position X. The N-terminal residues of the ion binding loop 1, including Val28, Leu29 and Gly30, are involved in unique conformational changes. From the 'disordered loop' conformation in the absence of ion binding, they adopt a helical conformation and become the C-terminal part of an extended helix A. These conformational changes, as well as a dramatic shift in the orientation of helix A results in the positioning of Gly30 O into a proximity and orientation to the bound Cd^{2+} for direct coordination.

Comparison of cNTnC EF 1 with non-canonical EF-hands

Calcium binding EF-hand proteins show significant diversity in the loop length and sequence composition of the calcium binding loop. Large differences are accommodated by adjustments within the backbone conformation such that the canonical coordination geometry is not changed. This frequently involves employing backbone carbonyl oxygens as the coordinating ligands. Like the cNTnC loop 1, the EF1 Ca²⁺ binding loop sequence of *Arabidopsis thaliana* calcineurin B-like protein (AtCBL2) (pdb: 1UHN)²⁶ is markedly different from the classical EF-hand loop. The N-terminal part of the loop is extended by two residues and it lacks the highly conserved aspartate residue in X- and Y- positions²⁶. It can nevertheless coordinate a Ca²⁺ ion in canonical pentagonal bipyramidal geometry. A unique mainchain conformation allows two mainchain backbone carbonyl oxygens to replace the canonical side chain carboxylate oxygens for the X- and Y- ligand positions. Similar to the structure presented here, the main chain carbonyl oxygen in the X-position comes from a residue in the entering helix.

The canonical and non-canonical Ca^{2+} binding loops nevertheless share a highly conserved C-terminus. Compared to the more dynamic N-terminal region, the C-terminal region is highly stabilized by the turn of the exiting helix and a hydrogen bond to the other ion binding loop of the paired EF-hand motif. This highly conserved sequence and structural features exist in the Cd^{2+} coordinating loop 1 of the structure presented here. First, the ligand in the -Y position is the main chain carbonyl oxygen (Cys35). This residue is then followed by a hydrophobic residue (Ile36), which is involved in β -sheet hydrogen bonding interaction with an equivalent residue (Val72) in the opposite loop (known as the 'EF β -scaffold'). The ligand at the -Z position is a bidentate interaction from a glutamate residue (Glu40) and there is a four residue spacing between the -Y and -Z ligands. The structural alignment of the backbone atoms of these conserved C-terminal residues in the loops of EF 1 (Asp33-Glu40) and EF 2 (Ser69-Glu76) results in a r.m.s.d of 1.2 Å.

The Cd²⁺ coordination by loop 1 lacks the extensive loop-stabilizing hydrogen-bond interactions in the Ca²⁺ coordinating EF-hand motifs between the residues that comprise the loop. EF 1 contains relatively few residues participating in Cd²⁺ coordination and the absence of chelating aspartate residues result in less extensive hydrogen bonding interactions as compared with EF 2. Moreover, the overall conformational change induced by the Cd²⁺ binding in loop 1 is uncharacteristic of NTnC. The Ca²⁺ binding in classical EFmotifs normally decrease the interhelical angle from ~135° to 90°. The Cd²⁺ induced conformational change in EF 1 is the opposite as the resulting interhelical angle increases to ~180° (~antiparallel helices). The rotation of helix A is approximately centred at Leu29. As a result, helix N and helix A have completely lost contact with helix D. The unusual antiparallel helical conformation adopted by the EF 1 appears similar to that of a non-Ca²⁺ binding EF-hand motif in the N-terminal EF-hand pair of recoverin²⁷. However, the helices are anti-parallel only in the Ca²⁺ free state of the protein. The Ca²⁺ binding by the other functional EF-hand motifs results in a conformational change which rotates the entering helix outward with marked changes in the interhelical angle²⁸. Thus, the conformational change observed in our structure is the opposite to that of recoverin and unique among available NTnC structures.

The binding of deoxycholic acid in the 'open' core

Deoxycholic acid (DXC), a by-product of intestinal bacteria, is a steroid acid commonly found in the bile of mammals (Figure 4A) $\frac{29}{2}$. DXC is used as a mild detergent for the isolation of membrane associated proteins³⁰ and was used for the optimization of the cNTnC crystallization condition. The inclusion of DXC resulted in crystals with a different morphology and spacegroup when compared to those grown without DXC. The electron density is consistent with two DXC molecules being associated with chain A (Figure 4B). One DXC molecule (DXC1) is present in the central hydrophobic cavity that is formed by a cluster of several hydrophobic residues. These include the aromatic ring of Phe27 from helix A, the side chains of Leu41, Val44, SeMet45 and Leu48 from helix B, and the side chains of Phe77 and SeMet81 from helix D. The calculated total surface area of the pocket is approximately 503Å². Electron density for DXC is present in all chains but the density is clearest in chain A. The hydrophobic fused rings of DXC are bound within the hydrophobic cavity while its carboxylate group is exposed to solvent. The other DXC molecule (DXC2) is bound to a hydrophobic patch on helix N and helix A. The details of its interaction differ in each chain. In chain A, the binding of this DXC molecule is stabilized by a ring stacking interaction with the aromatic ring of Phe24 and a hydrogen bonding interaction with the Lys17 Nζ of chain A. The carboxylate group of DXC also coordinates a Cd²⁺ ion with Glu59 $O^{\epsilon 1}$ and Glu59 $O^{\epsilon 2}$ of chain B.

The DXC molecule has similar features to the Ca^{2+} sensitizing drugs such as trifluoroperzaine (TFP) $\underline{^{23}}$, EMD 57033 $\underline{^{31}}$, and levosimendan $\underline{^{32}}$. They each have at least two hydrophobic fused rings and a hydrophilic head group. As listed below, structures in complex with these drugs show that the hydrophobic ring system binds to the hydrophobic pocket within TnC and the hydrophilic head group is often exposed to the solvent. The hydrophobicity and flexibility of the DXC appears to be an important feature for its interaction with cNTnC (Figure 4C).

Structural comparison with other cNTnC structures

Several of the drugs known as the Ca²⁺ sensitizers are used to treat heart failure, which is a condition characterized by the inability of the heart to supply sufficient blood flow to vital organs. The mechanisms utilized by these Ca²⁺ sensitizers vary widely, but in general they tend to increase the Ca²⁺ affinity of the troponin complex to improve cardiac muscle contractility without directly increasing the cytosolic Ca²⁺ concentration, which could potentially result in arrhythmia and diastolic dysfunction 34. Since the regulatory domain of cTnC serves an important role as a Ca²⁺ sensor, the structure of cNTnC in complex with a Ca²⁺-sensitizer molecule and the switch peptide of cTnI (cTnI ₁₄₇₋₁₆₃) has been investigated extensively in recent years. A number of the NMR and the crystal structures show that these Ca²⁺ sensitizers may function by binding to the hydrophobic cavity of cNTnC, stabilizing its open conformation, and thus facilitating the binding of cTnI to cNTnC. The overall conformation of cNTnC is very similar in all of these structures. They include the NMR structure of cNTnC in complex with a bepridil molecule and the cTnI₁₄₇₋₁₆₃ switch peptide (PDB: 1LX)35, the NMR structure of cNTnC in complex with a W7 molecule (PDB: $2KFX)^{36}$ and with both a W7 molecule and the $cTnI_{147-163}$ switch peptide (PDB: $2KRD)^{39}$, the NMR structure of cNTnC in complex with the cTnI₁₄₇₋₁₆₃ switch peptide and the analog

of levosimendan, 2',4'-difluorobiphenyl-4-yloxy acetic acid (dfbp-o) (PDB: 2L1R) $\frac{37}{2}$, and the crystal structure of cNTnC in complex with trifluoperazine (PDB: 1WRK) $\frac{23}{2}$. Using the best representative chain from each NMR ensemble and the single chain from 1WRK model, the superimposition of all the above mentioned structures yields a C_{α} r.m.s.d of 2.3 Å, indicating their similar overall conformation.

The presence of Ca^{2+} sensitizers and cTnI peptide in the hydrophobic pocket as well as Ca^{2+} binding to loop 2 induce the overall conformation of cNTnC to the 'open' state in these structures. Without these drugs, both the apo and Ca^{2+} bound state of cNTnC remain in the 'closed' state. The 'open' conformation of cNTnC is characterized by the helices B and C linked by a short linker moving away from the helices A and D resulting in the exposure of larger core hydrophobic surface area. The structure presented here resembles the 'open' conformation. This is due to the Cd^{2+} binding to loop 2 and the presence of DXC in the hydrophobic core, which is the prerequisite for the 'open' conformation in the other structures.

Discussions on the unique Cd²⁺ coordination in EF 1

The EF 1 of the mammalian cNTnC was shown to be incapable of Ca^{2+} binding over the range of physiological cytosolic Ca^{2+} concentration (100 - 2000 nM). This explains the different thermodynamic and kinetic responses to Ca^{2+} between cardiac TnC and skeletal TnC 11 . Therefore, finding a Cd^{2+} ion coordinated by residues from the defunct EF 1 in canonical ion coordination geometry is unexpected. In some respects, the Cd^{2+} binding in EF 1 resembles the metal ion coordination by versatile non-canonical EF-hands. As previously stated, the composition and length of their ion binding loops can vary significantly from the classical sequence yet the pentagonal bipyramid ion ligand coordination geometry can be maintained. This is made possible in part by the conserved 'scaffold' in the C-terminal part of the binding loops. The structure presented here indicates that such a scaffold is also conserved in EF 1 of cNTnC.

Without the dramatic conformational rearrangement by the helix A, the EF 1 ion coordination is unlikely to be reproduced. A simple extension of the helix A at the C-terminus while the helices N and A maintain contacts with helix D in the usual cNTnC conformation will result in the Gly30 O ligand pointing perpendicularly away from the bound ion. It is the perpendicular 'swing' of the helix A around the Leu29 hinge that brings the X - ligand into coordinating position. Therefore, the structure presented here does not necessarily imply that Ca²⁺ binding can occur at loop 1 in mammalian cNTnC. However, the conserved and structurally intact C-terminal part of the EF-hand motif alone is shown to provide 6 out of 7 required ligands in Y, Z, -Y, -X, -Z positions for canonical ion coordination (Figure 3C). Such a coordinating 'scaffold' probably played a role in stabilizing the considerable conformational change by cNTnC required for Cd²⁺ coordination in canonical geometry.

It is an interesting conundrum that the N-terminal region of loop 1 within the cNTnC domain in ectothermic species of vertebrates, particularly those adapted to survive at colder temperatures, have significantly different sequences. In trout cNTnC, the residues Ile28, Gln29, and Asp30 replace Val28, Leu29, Gly30 residues in human cNTnC (Figure 1B).

Moreover, they were found to be responsible for the comparatively higher Ca^{2+} affinity of trout cTnC compared to human cTnC $\frac{10}{}$. This in turn translates to higher Ca^{2+} sensitivity of trout cardiac myocytes which allows for normal trout cardiac function at its significantly lower physiological temperatures. These observations indicate unique but not well understood properties conferred by these residues towards the loop 1 of cNTnC and perhaps it may involve differential interaction with Ca^{2+} .

Previous NMR titration experiments suggested that Ca²⁺ binding can occur at EF 1 of trout cTnC in solution⁴⁰ albeit with a relatively low affinity. The structure presented here demonstrates that the intact C-terminus of loop 1 is capable of providing most of the required ion coordination, thus such binding may be possible with a favourable conformational change at the N-terminal part of the loop involving residues Ile28, Gln29, Asp30. It is probably more than coincidence that the corresponding three residues (Val28, Leu29, Gly30) in this human cNTnC structure are involved in the most significant disorder to order transition. Instead of the backbone carbonyl oxygen, perhaps the Asp30 side-chain carboxylate oxygen could provide the necessary coordination corresponding to the ligand in the X-position. Aspartic acid is the most favoured residue for the X-position in the ion binding loop of the EF-hand motif in general 16. If not a direct interaction, Asp30 may still be able to stabilize the Ca²⁺ binding via a water molecule or by forming a network of loopstabilizing hydrogen bonding interactions. The crystal structure presented here provides a snap shot of an unusual conformation of cNTnC that formed in the presence of Cd²⁺ and DXC molecule. The canonical coordination of Cd²⁺ demonstrates the preservation of functional elements in the C-terminal part of the vestigial loop that act as an important ion coordinating 'scaffold' in various EF-hand motifs.

Materials and Methods

Cloning and mutagenesis

The full length wild-type human cardiac TnC was cloned into the pET21a expression plasmid (Novagen) which was used to produce the cNTnC construct that contains residues 1-89. Lys90 was converted to a termination codon by site-directed mutagenesis using the Quick Change kit (Stratagene) with the 39-base forward primer 5'-TGTATGAAAGATGACAGCTAAGGAAAATCTGAAGAGGAG-3' and the reversed primer 5'-CTCCTCTTCAGATTTTCCTTAGCTGTCATCTTTCATACA – 3'. DNA sequencing (Marcogen) confirmed the cTnC sequence reported in the Swiss-Prot database (accession number P63316). The plasmid pET21a-cNTnC was transformed into BL21(DE3) *E. coli.* cells. The expressed protein (cNTnC) is 89 residues in length and has a calculated molecular mass of 10,062 Da and a theoretical isoelectric point of 4.0.

Protein over-expression and purification

Se-Met-incorporated protein was prepared by growing an overnight culture of BL21(DE3) transformed with the plasmid pET21a-cNTnC in M9 minimal medium supplemented with 100 μ g/mL ampicillin. 500 μ L of the overnight culture was used to inoculate 100 mL of M9 minimal medium (100 μ g/mL ampicillin) and 20 mL of that overnight M9 culture was used to inoculate 1 liter of M9 minimal media (100 μ g/mL ampicillin) that was grown for 5-6

hours at 37°C until the A 600 reached 0.6. Each liter of culture was then supplemented with the following combination of amino acids: 100 mg each of lysine, phenylalanine, threonine; 50 mg each of isoleucine, leucine, valine; 60 mg of L-selenomethionine. After 15 minutes, each liter of cell culture was induced with isopropyl-1-thio-β-galactopyranoside (IPTG) at a final concentration of 1 mM and grown for an additional 6 hours at 37°C. Cell pellets were then collected by centrifugation and resuspended with resuspension buffer (50 mM Tris-HCl pH 7.5, 25% sucrose, 0.5 mM PMSF, 2 mM MgCl₂) and EDTA-free 1 × protease inhibitor cocktail (Roche). Cells were completely lysed by sonicating three times with a five second interval at 30% amplitude using Model 500 Dismembrator (Fisher Scientific), and using an Avestin Emulsiflex-3C cell homogenizer. The supernatant was separated from the lysate by centrifugation at 2900 xg for 30 min. Final concentrations of 1 mM MgCl₂, 5 mM CaCl₂, 50 mM NaCl, and 1 mM DTT were added to the supernatant immediately after the centrifugation and the supernatant was then applied to a phenyl-sepharose 6 fast flow column (5 ml column volume, GE Health Care) equilibrated with a buffer consisting of: 50 mM Tris-HCl pH 7.5, 1 mM MgCl₂, 5 mM CaCl₂, 50 mM NaCl, and 1 mM DTT. The purification of cNTnC using the phenyl sepharose hydrophobic matrix was carried out as described by Li et. al. 41. The elution fractions containing cNTnC were concentrated using an Amicon ultracentrifuge filter device (Millipore) with a 3kDa MW cutoff. The protein was further purified by Sepharacryl S-100 HiPrep 26/60 size exclusion chromatography column on an AKTA Prime system (Pharmacia Biotech) that was run at 1 mL/min and equilibrated with 50 mM Tris-HCl pH 7.5, 0.2 mM CaCl₂, and 1 mM DTT. The fractions containing pure cNTnC were analyzed by 15% SDS-PAGE, combined, and concentrated to 10 mg/mL using an Amicon ultra-centrifuge filter device (Millipore) with a 3kDa cutoff and quantified by a NanoDrop Spectrophotometer ND-100.

Mass spectrometry analysis

To confirm the full incorporation of selenium atoms into the cNTnC protein, Matrix-Assisted Laser Desorption Ionization (MALDI) mass spectrometry was performed on a MALDI-LR time of flight (TOF) spectrometer (Waters Corp., Manchester, UK) in positive ion mode, using a matrix of sinapic acid saturated in 50% acetonitrile. The instrument was operated in linear mode with a pulse voltage = 1400 V, source voltage = 15,000 V, a multichannel plate detector potential difference of 1850 V and a TLF delay of 500 ns. Samples were desorbed with a nitrogen laser (1 = 337 nm) and the ion signals detected from 50 laser shots with sample times of 5 ns were summed for each mass spectrum archived. Mass spectra were recorded over an m/z range of 2000-20000. The proteins: myoglobin, cytochrome C, and adrenocorticotropic hormone fragment 18-39 (Sigma Chemical Co., St. Louis, MO, USA) were used as calibration standards.

Crystallization

The crystals used for single wavelength anomalous diffraction data collection were grown by the sitting-drop vapor diffusion method. The crystallization drops were prepared by mixing 1 μ L of purified protein (10 mg/mL) with 1 μ L of reservoir solution and 1 μ L of 50 mM deoxycholic acid then equilibrating against 1 mL of reservoir solution. The optimized crystallization reservoir condition contained 50 mM CdSO₄, 900 mM sodium acetate, and 100 mM Tris-HCl (pH 8.0). The long plate-shaped crystals were grown at room temperature

(293 K) and optimized crystals appeared after three days. Prior to data collection, crystals were transferred to a cryoprotectant solution, which consisted of the same components as the reservoir solution but with 30% of the water replaced with glycerol. Crystals were incubated in the cryoprotectant solution for approximately 10 minutes before they were flash cooled in liquid nitrogen.

Data collection

Diffraction data from the Se-Met-incorporated wild-type cNTnC crystals were performed at Beamline 081D-1 of the Canadian Light Source, Canadian Macromolecular Crystallography Facility, University of Saskatchewan at Saskatoon using the Mar 225 CCD X-ray detector. Se-Met data set 1 (used for heavy atom search) was collected with a crystal-to-detector distance of 180 mm and a 1° oscillation. A total of 180 images were collected. Reflections were detectable up to 2.1 Å resolution. Se-Met data set 2 (used for structural refinement) was collected with a crystal-to-detector distance of 180 mm and 1° of oscillations. A total of 150 images were collected. The reflections were detectable to 2.2 Å.

Phasing, structure determination, and refinement

Se-Met data set 1 collected at a wavelength $\lambda = 0.98086$ was used for phase calculation by the single wavelength anomalous dispersion (SAD) method. Diffraction images were processed with HKL3000. The merging of data sets and corrections for radiation-induced effects were performed using a novel hierarchical procedure ¹⁸, ⁴⁵. Heavy atom position search was performed at 2.8 Å with SHELXD⁴⁶. The map generated by SHELXE had clearly interpretable electron density and was subsequently used for the initial model building with ARP/wARP. The refinement of heavy atoms positions and the further phasing was performed with MLPHARE 48, which resulted in 28 refined heavy atom positions. This phase information was used in the model building and refinement as an additional restraint. Intensities from SeMet data set 2 collected at wavelength $\lambda = 0.98066$ were used for structure refinement with the program REFMAC5⁴⁹. Subsequent manual model building by visual inspection of the electron density map was carried out using COOT⁵². The final models were obtained by running restrained refinement with Translation Liberation Screw Rotation (TLS) restraints obtained from the TLS motion determination server⁵⁰. The complete data collection and refinement statistics are in Table 1. The structural coordinate and structure factors have been deposited in the RCSB Protein Data Bank (PDB ID: 3RV5).

Structural Analysis

The secondary structural analysis was performed with the programs DSSP⁵¹ and PROMOTIF⁵². The programs Coot⁵³ and SUPERPOSE⁵⁴ were used to overlap coordinates for structural comparison. The stereochemistry of the structure was analyzed with the program PROCHECK⁵⁵. B-factor analysis was performed by the program BAVERAGE within the CCP4 suite of programs⁵⁶.

Figure Preparation

Figures were prepared using PyMOL⁵⁷. The alignment figure was prepared using the programs ClustalW⁵⁸. The chemical structure of deoxycholate was drawn by GCChemPaint⁵⁹.

Supplementary Material

Refer to Web version on PubMed Central for supplementary material.

Acknowledgments

This work was supported by a Grant-in-Aid from the Heart and Stroke Foundation of British Columbia and Yukon (GFT/MP) and operating grants from the Canadian Institutes of Health Research (CIHR) and the Natural Science and Engineering Research Council (NSERC) of Canada awarded to MP. MP is a scholar of the Michael Smith Foundation for Health Research and GFT is a Canada Research Chair. We thank the staff at the macromolecular beam line 08ID-1, Canadian Light Source, Saskatoon, Canada for their technical assistance with data collection. The Canadian Light Source is supported by NSERC, NRC, CIHR, and the University of Saskatchewan.

Abbreviations

cTnC cardiac troponin C

cNTnC amino-terminal domain of cardiac troponin C

DXC deoxycholic acid

EF 1 EF-hand motif 1

EF 2 EF-hand motif 2

ASU Asymmetric Unit

Reference

- 1. Farah CS, Reinach FC. The troponin complex and regulation of muscle contraction. Faseb J. 1995; 9:755–67. [PubMed: 7601340]
- 2. Gordon AM, Homsher E, Regnier M. Regulation of contraction in striated muscle. Physiol Rev. 2000; 80:853–924. [PubMed: 10747208]
- 3. Kretsinger RH, Nockolds CE. Carp muscle calcium-binding protein. II. Structure determination and general description. J Biol Chem. 1973; 248:3313–26. [PubMed: 4700463]
- 4. Strynadka NC, James MN. Crystal structures of the helix-loop-helix calcium-binding proteins. Annu Rev Biochem. 1989; 58:951–98. [PubMed: 2673026]
- 5. van Eerd JP, Takahashi K. The amino acid sequence of bovine cardiac tamponin-C. Comparison with rabbit skeletal troponin-C. Biochem Biophys Res Commun. 1975; 64:122–7. [PubMed: 1170846]
- 6. Li MX, Gagne SM, Spyracopoulos L, Kloks CP, Audette G, Chandra M, Solaro RJ, Smillie LB, Sykes BD. NMR studies of Ca2+ binding to the regulatory domains of cardiac and E41A skeletal muscle troponin C reveal the importance of site I to energetics of the induced structural changes. Biochemistry. 1997; 36:12519–25. [PubMed: 9376356]
- 7. Teleman O, Drakenberg T, Forsen S, Thulin E. Calcium and cadmium binding to troponin C. Evidence for cooperativity. Eur J Biochem. 1983; 134:453–7. [PubMed: 6309513]
- 8. Holroyde MJ, Robertson SP, Johnson JD, Solaro RJ, Potter JD. The calcium and magnesium binding sites on cardiac troponin and their role in the regulation of myofibrillar adenosine triphosphatase. J Biol Chem. 1980; 255:11688–93. [PubMed: 6449512]

 Spyracopoulos L, Gagne SM, Li MX, Sykes BD. Dynamics and thermodynamics of the regulatory domain of human cardiac troponin C in the apo- and calcium-saturated states. Biochemistry. 1998; 37:18032–44. [PubMed: 9922172]

- 10. Gillis TE, Liang B, Chung F, Tibbits GF. Increasing mammalian cardiomyocyte contractility with residues identified in trout troponin C. Physiol Genomics. 2005; 22:1–7. [PubMed: 15784699]
- 11. Gillis TE, Marshall CR, Tibbits GF. Functional and evolutionary relationships of troponin C. Physiol Genomics. 2007; 32:16–27. [PubMed: 17940202]
- Hoffmann B, Schmidt-Traub H, Perrot A, Osterziel KJ, Gessner R. First mutation in cardiac troponin C, L29Q, in a patient with hypertrophic cardiomyopathy. Hum Mutat. 2001; 17:524. [PubMed: 11385718]
- 13. Putkey JA, Dotson DG, Mouawad P. Formation of inter- and intramolecular disulfide bonds can activate cardiac troponin C. J Biol Chem. 1993; 268:6827–30. [PubMed: 8463206]
- 14. Li Y, Love ML, Putkey JA, Cohen C. Bepridil opens the regulatory N-terminal lobe of cardiac troponin C. Proc Natl Acad Sci U S A. 2000; 97:5140–5. [PubMed: 10792039]
- 15. Grabarek Z. Structural basis for diversity of the EF-hand calcium-binding proteins. J Mol Biol. 2006; 359:509–25. [PubMed: 16678204]
- 16. Gifford JL, Walsh MP, Vogel HJ. Structures and metal-ion-binding properties of the Ca2+-binding helix-loop-helix EF-hand motifs. Biochem J. 2007; 405:199–221. [PubMed: 17590154]
- 17. Borek D, Ginell SL, Cymborowski M, Minor W, Otwinowski Z. The many faces of radiation-induced changes. J Synchrotron Radiat. 2007; 14:24–33. [PubMed: 17211069]
- Borek D, Cymborowski M, Machius M, Minor W, Otwinowski Z. Diffraction data analysis in the presence of radiation damage. Acta Crystallogr D Biol Crystallogr. 2010; 66:426–36. [PubMed: 20382996]
- Rao ST, Satyshur KA, Greaser ML, Sundaralingam M. X-ray structures of Mn, Cd and Tb metal complexes of troponin C. Acta Crystallogr D Biol Crystallogr. 1996; 52:916–22. [PubMed: 15299599]
- 20. Forsen S, Thulin E, Lilja H. 113Cd NMR in the study of calcium binding proteins: troponin C. FEBS Lett. 1979; 104:123–6. [PubMed: 477971]
- Dokmanic I, Sikic M, Tomic S. Metals in proteins: correlation between the metal-ion type, coordination number and the amino-acid residues involved in the coordination. Acta Crystallogr D Biol Crystallogr. 2008; 64:257–63. [PubMed: 18323620]
- 22. Takeda S, Yamashita A, Maeda K, Maeda Y. Structure of the core domain of human cardiac troponin in the Ca(2+)-saturated form. Nature. 2003; 424:35–41. [PubMed: 12840750]
- 23. Takeda S, Igarashi T, Oishi Y, Mori H. Crystal structure of the N-terminal domain of human cardiac troponin C in complex with trifluoperazine. 2004 To be Published.
- 24. Akke M, Forsen S, Chazin WJ. Solution structure of (Cd2+)1-calbindin D9k reveals details of the stepwise structural changes along the Apo-->(Ca2+)II1-->(Ca2+)I,II2 binding pathway. J Mol Biol. 1995; 252:102–21. [PubMed: 7666423]
- Andersen O. Chelation of cadmium. Environ Health Perspect. 1984; 54:249–66. [PubMed: 6734560]
- Nagae M, Nozawa A, Koizumi N, Sano H, Hashimoto H, Sato M, Shimizu T. The crystal structure of the novel calcium-binding protein AtCBL2 from Arabidopsis thaliana. J Biol Chem. 2003; 278:42240–6. [PubMed: 12871972]
- Tanaka T, Ames JB, Harvey TS, Stryer L, Ikura M. Sequestration of the membrane-targeting myristoyl group of recoverin in the calcium-free state. Nature. 1995; 376:444–7. [PubMed: 7630423]
- Ames JB, Ishima R, Tanaka T, Gordon JI, Stryer L, Ikura M. Molecular mechanics of calciummyristoyl switches. Nature. 1997; 389:198–202. [PubMed: 9296500]
- 29. Hofmann AF. The continuing importance of bile acids in liver and intestinal disease. Arch Intern Med. 1999; 159:2647–58. [PubMed: 10597755]
- 30. Neugebauer JM. Detergents: an overview. Methods Enzymol. 1990; 182:239–53. [PubMed: 2314239]

31. Wang X, Li MX, Spyracopoulos L, Beier N, Chandra M, Solaro RJ, Sykes BD. Structure of the C-domain of human cardiac troponin C in complex with the Ca2+ sensitizing drug EMD 57033. J Biol Chem. 2001; 276:25456–66. [PubMed: 11320096]

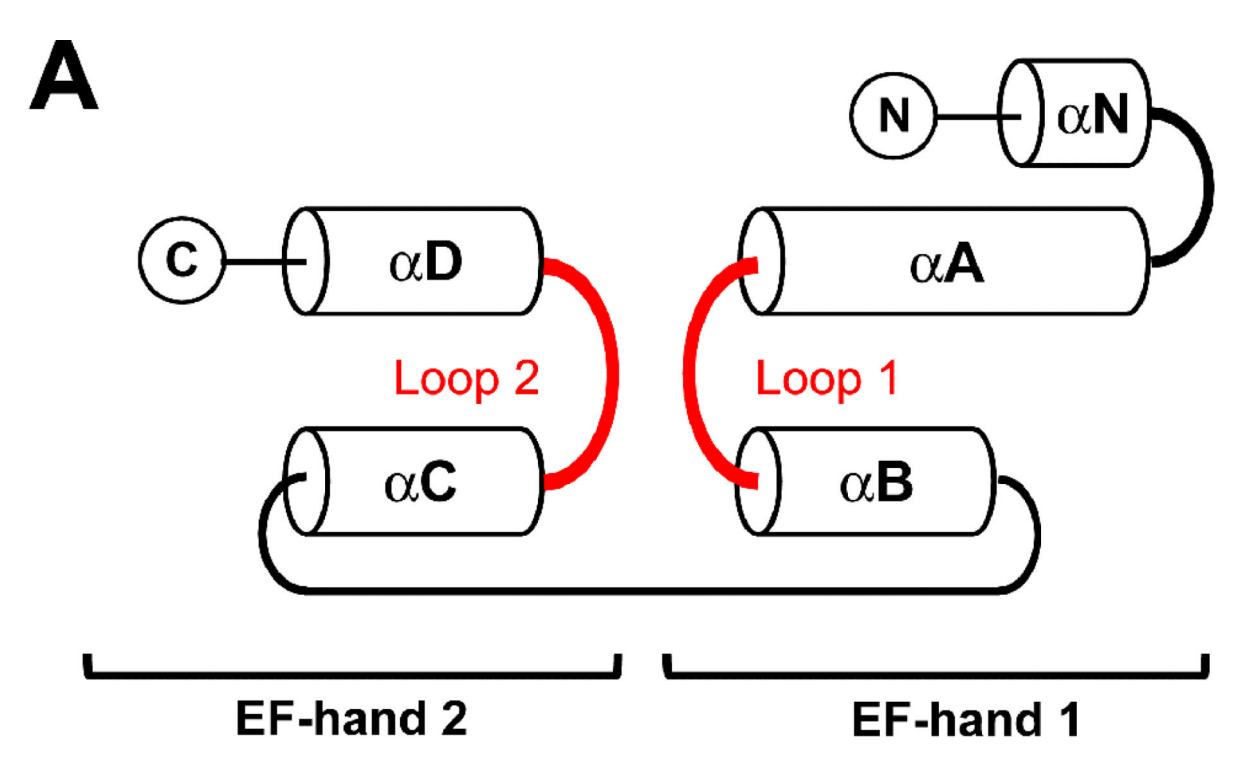
- 32. Robertson IM, Baryshnikova OK, Li MX, Sykes BD. Defining the binding site of levosimendan and its analogues in a regulatory cardiac troponin C-troponin I complex. Biochemistry. 2008; 47:7485–95. [PubMed: 18570382]
- 33. Endoh M. Could Ca2+ sensitizers rescue patients from chronic congestive heart failure? Br J Pharmacol. 2007; 150:826–8. [PubMed: 17325657]
- 34. Kass DA, Solaro RJ. Mechanisms and use of calcium-sensitizing agents in the failing heart. Circulation. 2006; 113:305–15. [PubMed: 16418450]
- 35. Wang X, Li MX, Sykes BD. Structure of the regulatory N-domain of human cardiac troponin C in complex with human cardiac troponin I147-163 and bepridil. J Biol Chem. 2002; 277:31124–33. [PubMed: 12060657]
- 36. Hoffman RM, Sykes BD. Structure of the inhibitor W7 bound to the regulatory domain of cardiac troponin C. Biochemistry. 2009; 48:5541–52. [PubMed: 19419198]
- 37. Robertson IM, Sun YB, Li MX, Sykes BD. A structural and functional perspective into the mechanism of Ca(2+)-sensitizers that target the cardiac troponin complex. J Mol Cell Cardiol. 2010
- 38. Li MX, Robertson IM, Sykes BD. Interaction of cardiac troponin with cardiotonic drugs: a structural perspective. Biochem Biophys Res Commun. 2008; 369:88–99. [PubMed: 18162171]
- 39. Oleszczuk M, Robertson IM, Li MX, Sykes BD. Solution structure of the regulatory domain of human cardiac troponin C in complex with the switch region of cardiac troponin I and W7: the basis of W7 as an inhibitor of cardiac muscle contraction. J Mol Cell Cardiol. 2010; 48:925–33. [PubMed: 20116385]
- 40. Gillis TE, Blumenschein TM, Sykes BD, Tibbits GF. Effect of temperature and the F27W mutation on the Ca2+ activated structural transition of trout cardiac troponin C. Biochemistry. 2003; 42:6418–26. [PubMed: 12767223]
- 41. Li MX, Chandra M, Pearlstone JR, Racher KI, Trigo-Gonzalez G, Borgford T, Kay CM, Smillie LB. Properties of isolated recombinant N and C domains of chicken troponin C. Biochemistry. 1994; 33:917–25. [PubMed: 8305439]
- 42. Minor W, Cymborowski M, Otwinowski Z, Chruszcz M. HKL-3000: the integration of data reduction and structure solution--from diffraction images to an initial model in minutes. Acta Crystallogr D Biol Crystallogr. 2006; 62:859–66. [PubMed: 16855301]
- 43. Otwinowski, Z.; Minor, W. Processing of X-ray Diffraction Data Collected in Oscillation Mode.. In: C.W. Carter, J.; Sweet, RM., editors. Methods Enzymol. Vol. 276. Academic Press; 1997. p. 307-326.
- 44. Otwinowski, Z.; Minor, W. Denzo and Scalepack. In International Tables for Crystallography. Rossman, MG., editor. Vol. F. Kluwer Academic Publishers; Dordrecht: 2000. p. 226p. 235
- 45. Tikhonov, AN.; Arsenin, VY. Solutions of ill-posed problems. Winston and Sons distributed by Wiley and Sons; New York: 1977.
- 46. Sheldrick GM. A short history of SHELX. Acta Crystallogr A. 2008; 64:112–22. [PubMed: 18156677]
- 47. Perrakis A, Sixma TK, Wilson KS, Lamzin VS. wARP: Improvement and extension of crystallographic phases by weighted averaging of multiple-refined dummy atomic models. Acta Crystallographica Section D-Biological Crystallography. 1997; 53:448–455.
- 48. Otwinowski Z. Maximum likelihood refinement of heavy atom parameters. CCP4 Study Weekend Proceedings Isomorphous Replacement And Anomalous Scattering. 1991:80–87.
- 49. Winn MD, Isupov MN, Murshudov GN. Use of TLS parameters to model anisotropic displacements in macromolecular refinement. Acta Crystallogr D Biol Crystallogr. 2001; 57:122–33. [PubMed: 11134934]
- Painter J, Merritt EA. Optimal description of a protein structure in terms of multiple groups undergoing TLS motion. Acta Crystallogr D Biol Crystallogr. 2006; 62:439–50. [PubMed: 16552146]

51. Kabsch W, Sander C. Dictionary of protein secondary structure: pattern recognition of hydrogen-bonded and geometrical features. Biopolymers. 1983; 22:2577–637. [PubMed: 6667333]

- 52. Hutchinson EG, Thornton JM. PROMOTIF--a program to identify and analyze structural motifs in proteins. Protein Sci. 1996; 5:212–20. [PubMed: 8745398]
- 53. Emsley P, Cowtan K. Coot: model-building tools for molecular graphics. Acta Crystallogr D Biol Crystallogr. 2004; 60:2126–32. [PubMed: 15572765]
- 54. Maiti R, Van Domselaar GH, Zhang H, Wishart DS. SuperPose: a simple server for sophisticated structural superposition. Nucleic Acids Res. 2004; 32:W590–4. [PubMed: 15215457]
- 55. Laskowski RA, MacArthur MW, Moss DS, Thornton JM. PROCHECK: a program to check the stereochemical quality of protein structures. J. Appl. Crystallogr. 1993; 26:283–291.
- 56. Number 4, C. C. P. The CCP4 suite: programs for protein crystallography. Acta Crystallogr D Biol Crystallogr. 1994; D50:760–763.
- 57. DeLano, WL. DeLano Scientific. San Carlos, CA, USA: 2002. The PyMol molecular graphics system..
- 58. Thompson JD, Higgins DG, Gibson TJ. Improved sensitivity of profile searches through the use of sequence weights and gap excision. Comput Appl Biosci. 1994; 10:19–29. [PubMed: 8193951]
- 59. Brefort J. GChemPaint 0.8.7. 2001

Article: YJMBI 63271 Highlights

- > The crystal structure of wild-type human cNTnC was determined to 2.2 Å resolution.
- > cNTnC binds Cd²⁺ in its two EF-hand ion binding loops.
- > The cNTnC vestigial Ca $^{2+}$ binding site coordinates a Cd $^{2+}$.
- > Deoxycholate is bound in the cNTnC central hydrophobic cavity.
- > cNTnC has a unique conformational when in complex with Cd²⁺ and deoxycholate.



В				Loop 1		
	Human	24	FDIF	VLGAEDGCISTKE	LGKV	
	Chicken	24	FDIF	VLGAEDGCISTKE	LGKV	cardiac TnC
	Trout	24	FDIF	IQDAEDGCISTKE	LGKV	
	Human Chicken	24 27	FDMF	-DADGGGDISVKE -DADGGGDISTKE	LGTV LGTV	skeletal TnC
	Salmon	24	FDMF	-DTDGGGDISTKE	LGTV	

Figure 1.

The topology of NTnC and the sequence variability observed within loop 1. (A) NTnC is comprised of five α -helices that are labeled N, A, B, C, D. The five α -helices assemble into two helix-loop-helix motifs (EF-hand motifs). EF-hand 1 is composed of helices αA , βB and loop 1 (red), EF-hand 2 is composed of αC and αD and loop 2 (red). (B) A sequence alignment of ion binding loop 1 (boxed) and surrounding residues in the first EF-hand motif of NTnC. The cardiac NTnC sequences shown are those from human (Swiss-Prot accession number: P63316), chicken (P09860), and trout cNTnC (Q7ZZB9). The skeletal NTnC

sequences are those of human (P02585), chicken (P02588) and Atlantic salmon (B9EP57). The residues conserved throughout are colored in red for cardiac TnC and blue for skeletal TnC. The skeletal NTnC loop 1 residues that coordinate Ca^{2+} are indicated by stars.

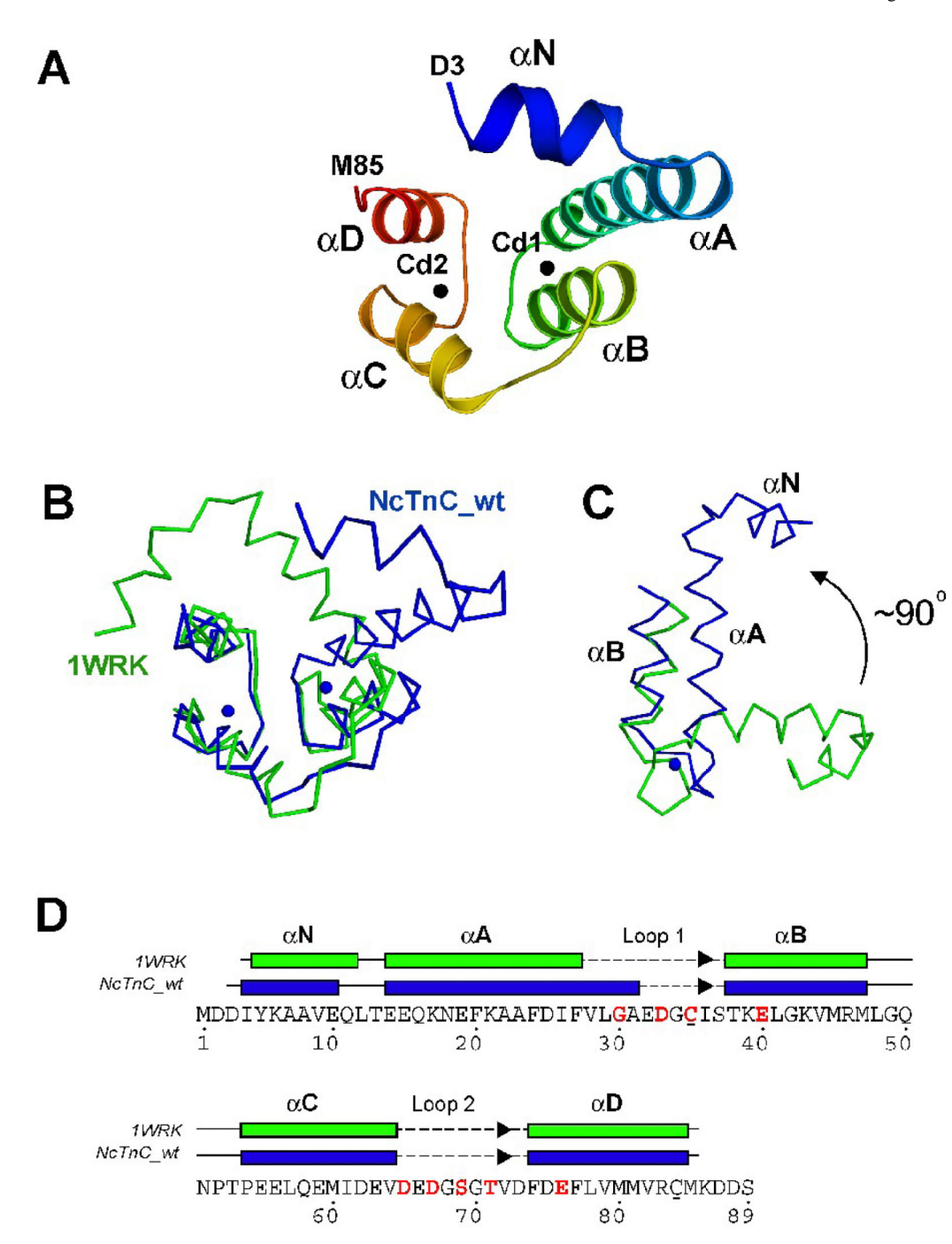
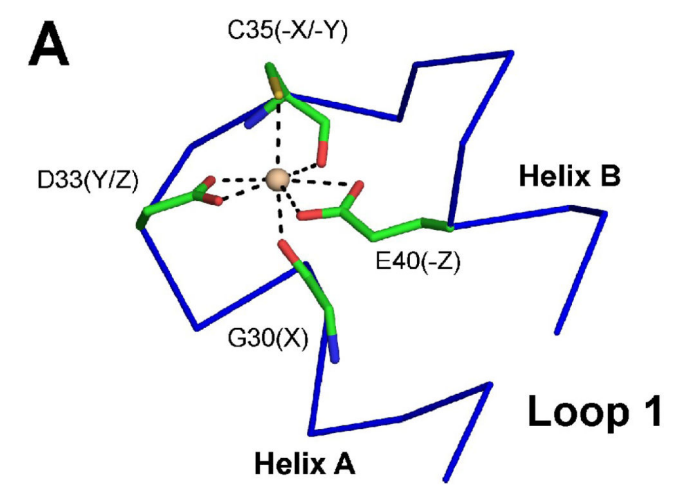
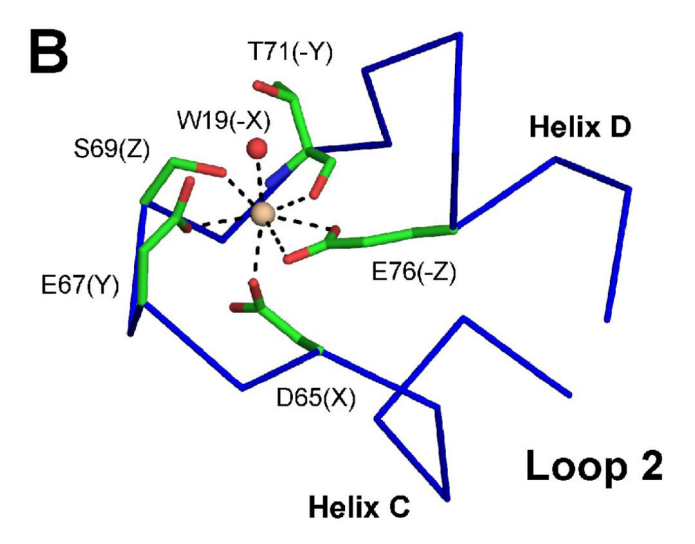


Figure 2. The protein fold of human cNTnC with structural comparisons. (A). A cartoon rendering of human cNTnC (Chain A) is colored spectrally from the N-terminus (blue) to the C-terminus (red). The amino- and carboxyl-termini and five helices N, A, B, C, D are labeled. The Cd²⁺ ions coordinated by the ion binding loops are shown as black spheres. (B) Chain A of human wild-type cNTnC (blue) is superimposed with human cNTnC (C35S and C84S mutant) complexed with trifluoperazine (PDB: 1WRK) (green). The bound Cd²⁺ ions are shown as blue spheres. (C). The comparison of the first EF-hand motif in the superimposed structures.

The major structural difference is the relative position of helix N and helix A with respect to helix B. There is a $\sim 90^\circ$ shift in this region of the structure when compared to 1WRK. (**D**). The secondary structure elements of this human cNTnC chain A (blue) and 1WRK are overlaid with the sequence of human cNTnC. The arrows indicate the mainchain hydrogen bond formed between Ile35 and Val72. The residues that coordinate Cd^{2+} in this structure are colored in red. The Cys35 and Cys84 residues mutated to serine in 1WRK are underlined.





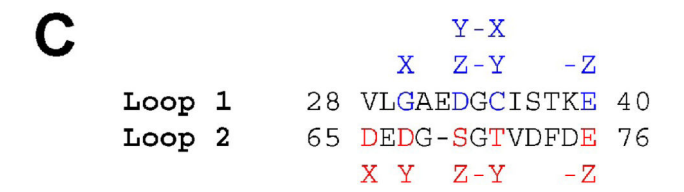
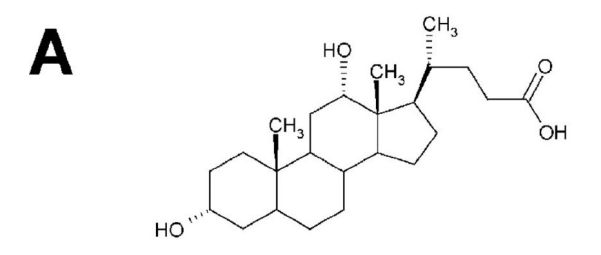
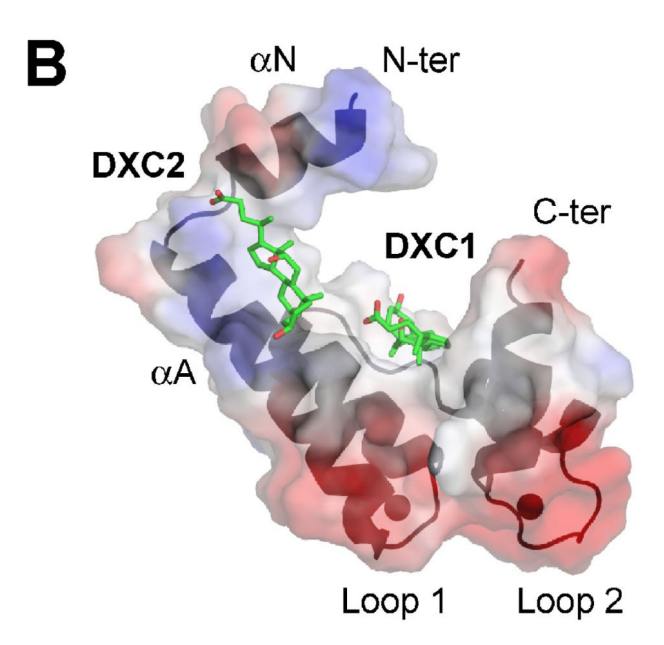


Figure 3.

The coordination of Cd^{2+} ions in human cNTnC. The residue sidechains that are directly involved in the Cd^{2+} coordination are shown in stick (carbon: green, oxygen: red). The protein mainchain is shown as blue $C\alpha$ trace. The water molecule is shown as a red sphere and the Cd^{2+} ions are shown as larger wheat colored spheres. (**A**) Cd^{2+} coordination in pentagonal bipyramidal geometry in the non-canonical loop 1 of EF 1. (**B**) A canonical Cd^{2+} coordination in loop 2 of EF 2. (**C**) The amino acid sequence for EF 1 loop1 (residues 28-40) and EF 2 loop2 (residues 65-76) are aligned and the residues involved in ion

coordination are colored in blue (loop 1) and in red (loop 2). The ligand coordination positions for the participating residues are indicated in the same color.





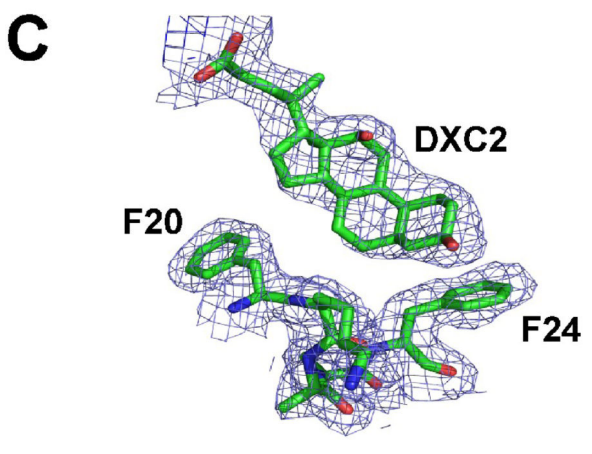


Figure 4. Deoxycholic acid (DXC) binding interactions with human cNTnC. (A) The chemical structure of DXC. (B) DXC binding sites on cNTnC. DXC is shown in stick format and cNTnC (chain A) is rendered as semitransparent surface with mapped electrostatic surface. (White: neutral; blue: positive; red: negative). DXC1 is bound at the central hydrophobic cavity while DXC2 is bound between αN and αA . (C) A sample of the $2F_0$ - F_c electron

density map contoured at 1.0 σ is shown for residues Phe20 to Phe24 of chain A and the nearby DXC2.

Table 1

Data collection, phasing, and refinement statistics

Crystal parameters	a	Se-Met Data 2		
	Se-Met Data 1 ^a			
Space group	P2 ₁ 2 ₁ 2	P2 ₁ 2 ₁ 2		
a, b, c (Å)	51.8, 81.8, 100.5	51.8, 81.8, 100.5		
Data collection statistics	i			
Wavelength	0.98068	0.98066		
Resolution (Å)	2.5-50.0 (2.5-2.6) ^b	2.2-50.0 (2.2-2.3)		
Total reflection	75935	85499		
Unique reflection	14864 (1414)	22061 (2192)		
R _{merge}	0.081 (0.091)	0.067 (0.176)		
Mean (I)/σ(I)	26.2 (4.1)	28.4 (5.7)		
Completeness	95.5 (93.8)	98.4 (99.1)		
Redundancy	4.0 (3.4)	3.9 (3.8)		
Phasing statistics				
Overall FOM	0.23			
Refinement statistics				
Protein molecules in AU	4			
Residues	322			
Water molecule	133			
Total number of atoms	2815			
Number of deoxycholate ions	5			
Number of cadmium ions	21			
Number of calcium ions	3			
$R_{\text{cryst}}^{d}/R_{\text{free}}^{e}$ (%)	22.5 / 28.1			
Average <i>B</i> -factor (Å ²)	41.3			
r.m.s.d on angles (°)	1.89			
r.m.s.d on bonds (Å)	0.03			
Ramachandran analysis (%)				
Preferred regions	271 (96.1 %)			
Allowed regions	11 (3.9 %)			
Outliers	0 (0.00%)			
B-factor				
Overall	41.3			
N-cTnC chain A	35.2			
N-cTnC chain B	37.8			
N-cTnC chain C	47.1			
N-cTnC chain D	44.1			

Crystal parameters	Se-Met Data 1 ^a	Se-Met Data 2			
Deoxycholate ions	58.5				
Cadmium ions	39.3				
Calcium ions	57.6				
Water molecules	27.5				
Residues missing from the models due to a lack of electron density					
Chain A	1-2, 86-89				
Chain B	1-4, 83-89				
Chain C	1-2, 86-89				
Chain D	1-4, 83-89				

 $[^]a$ Se-Met Data 1 was used to obtain initial phase estimates and Se-Met Data 2 was used for structure refinement.

 $[\]ensuremath{^b}\xspace$ The data collection statistics in brackets are the values for the highest resolution shell.

 $^{^{}C}R_{merge} = \Sigma_{hkl}\Sigma_{i}|I_{i}(hkl) - \langle I(hkl)\rangle| / \Sigma_{hkl}\Sigma_{i}I_{i}(hkl)$, where $I_{i}(hkl)$ is the intensity of an individual reflection and $\langle I(hkl)\rangle$ is the mean intensity of that reflection.

 $d_{\textit{R}_{\textit{CTYST}}} = \Sigma_{\textit{hkl}} \| F_{\textit{ObS}} | - |F_{\textit{Calc}}\| \ / \ \Sigma_{\textit{hkl}} | F_{\textit{ObS}}|, \text{ where } F_{\textit{ObS}} \text{ and } F_{\textit{Calc}} \text{ are the observed and calculated structure-factor amplitudes, respectively.}$

 $[^]e\mathrm{R}_{\mbox{free}}$ is calculated using 5% of the reflections randomly excluded from refinement.

 Table 2

 Canonical cadmium ion coordination by loop 1 and loop 2 in wild-type N-cTnC chain A

		Loop	1	Loop 2		
Position	Residue	Atom	Distance [Å]	Residue	Atom	Distance [Å]
	Val28					
	Leu29					
X	Gly30	0	2.2	Asp65	Οδ2	2.1
	Ala31			Glu66		
	Glu32					
Y	Asp33	Οδ1	2.4	Asp67	Οδ1	2.3
				Gly68		
Z	Asp33	Οδ2		Ser69	Оγ	2.3
	Gly34			Gly70		
-Y	Cys35	0	2.5	Thr71	0	2.4
-X	Cys35	s	2.5	W15	0	2.3
	Ile36			Val72		
	Ser37			Asp73		
	Thr38			Phe74		
	Lys39			Asp75		
-Z	Glu40	Οε1 Οε2	2.4 2.6	Glu76	Οε1 Οε2	2.3 2.6